

Definition of the Border Between the Far and Near Field Zone for Printed Antenna Arrays with High Side Lobe Suppression

Marija Milijić¹, Aleksandar Nešić², Bratislav Milovanović¹

Abstract: The paper defines the border between the far and near field zone of printed antenna arrays. The conventional definition has a limited application in side lobe suppression measurements, especially in the case of high side lobe suppression. The paper particularly details the printed antenna array with 8 radiation elements. Its symmetrical tapered feed network with Chebyshev distribution enables side lobe suppression greater than -44 dB in the E-plane. In addition, the influence of tolerances in the standard photolithographic process has been investigated. The expected tolerances in the standard photolithographic process have been assumed with moderate precision in order to estimate the side lobe suppression degradation due to amplitude and phase deviations, as well as deviations to optimized values in radiating element positioning.

Keywords: Printed antenna array, Side lobe suppression, Near and far field.

1 Introduction

The border between the far and near field is the distance from the antenna where the radiation pattern equals the mentioned in infinity. The clear border is undeterminable if the side lobe position, the gain and 3 dB beam width are important. The border and side lobe suppression (SLS) greatly depend on the applied distribution in the antenna array.

The usually used well-known formula is $L = 2D^2/\lambda$, where D is the largest antenna dimension. This formula can be used for antennas with uniform distribution that corresponds to the side lobe suppression of 13 dB. Meanwhile, antenna arrays with a tapered distribution are characterized by the distance to the border between the far and near field, which is a multiple of $2D^2/\lambda$, dependent on the applied distribution type and pedestal [1]. The following distributions were considered: uniform (referential), cosine-squared (-32 dB), Hanning (-42 dB), modified Taylor (-50 dB), Chebishev (-40 dB) and Chebyshev (-60 dB) [1]. However, one important factor that influences side

¹University of Niš, Faculty of Electronic Engineering Niš, Aleksandra Medvedeva 14, 18000 Niš, Serbia; E-mails: marija.milijic@elfak.ni.ac.rs, bratislav.milovanovic@elfak.ni.ac.rs

²IMTEL-komunikacije a.d., Bulevar Mihaila Pupina 165b, 11070 Novi Beograd, Serbia; E-mail: aca@insintel.com

lobe suppression is the distance between the radiation elements. The reference [1] considered the standard distance of $\lambda/2$ between the radiation elements. The research [1] was conducted to measure radar antenna AWACS, which has been the most demanding measurement to date.

With the use of LINPLAN [2] software, this paper will investigate a few usually applied distributions: Dolph-Chebyshev, Taylor and cosine, with a different number of radiating elements and different distance between the radiating elements. The focus will be on side lobe suppression between 30 dB and 40 dB (Low sidelobe), as well as side lobe suppression above 40 dB (Ultralow sidelobes). The variables are: the number of the array's radiating elements, distribution pattern and distance between the radiating elements. The paper especially analyzes the measure of side lobe suppression of the antenna array that is being realized. With 8 radiating elements, it applies the Dolph-Chebyshev distribution of 2.2 orders with a pedestal of -19 dB, resulting in the side lobe suppression of -44.8 dB (without realization errors).

2 The Method of Defining the Far Field Zone, Based on the Simulation Radiation Pattern with Phase Errors that Depend on the Measuring Antenna Distance

Fig. 1 shows an antenna array with n radiation elements at distance l . The experimental verification of the antenna array's radiation pattern requires the necessary measures in the far radiation field. Formula $L = 2D^2/\lambda$ is usually used to determine the border between the far and near field radiation zone. In this case, the biggest phase error is 22.5° for distance L and $L + \Delta\delta_i$, where $i = 1$ and n [3]. It is necessary to consider the phase errors of certain array elements, compared to the array center at distance L (Fig. 1), especially for measuring the side lobe suppression above -30 dB. If LINPLAN [2] software calculates the side lobe suppression, including the expected phase errors from certain array elements, the radiation pattern can be significantly changed. Consequently, it is necessary to determine distance kL , $k = 1, 2, \dots$, where the difference between the expected radiation pattern and the radiation pattern, including the phase errors of array elements $\Delta\delta_i$, $i = 1, 2, \dots, n$, is acceptable. The phase errors resulting from certain array elements depend on their position and on distance kL , $k = 1, 2, \dots$, where the measurement should be done. The phase errors $\Delta\delta_i$, $i = 1, 2, \dots, n/2$ from radiating elements in the symmetrical antenna array are defined in the following manner:

$$\Delta\delta_i = \Delta\delta_{n-i+1} = \frac{360}{\lambda} \left(\sqrt{(kL)^2 + \frac{l^2}{4}(n-2i+1)^2} - kL \right). \quad (1)$$

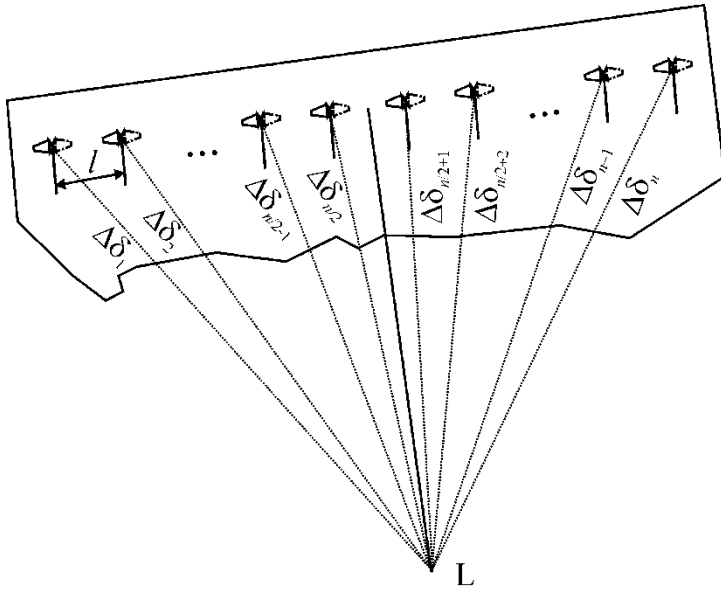


Fig. 1 – Antenna array with n radiation elements.

3 The influence of Antenna Array Parameters on the Definition of the Border Between the Far and Near Field Zone

The linear antenna array at the central frequency of 12 GHz will be considered in the following text. The array elements are positioned at constant distance l . The plane reflector in the dimensions of (240×52) mm is situated behind the array, at distance $\lambda/4 = 6.25$ mm (Fig. 2).

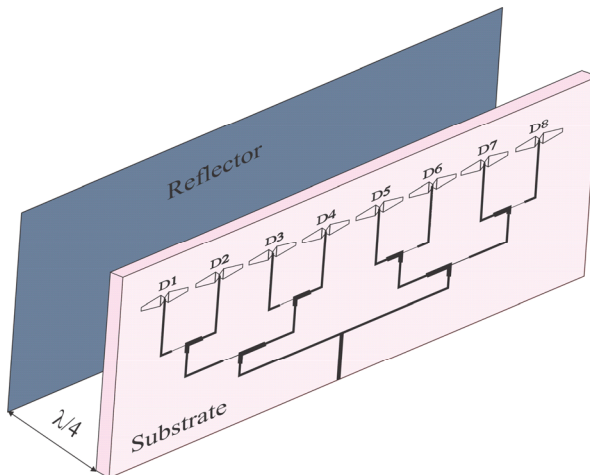


Fig. 2 – Antenna array with 8 radiation elements.

3.1 The influence of antenna array distribution on the definition of the border between the far and near field zone

The influence of antenna distribution on the definition of the border between the far and near field zone considered for the array consists of 8, 10 or 12 radiating elements at the uniform distance of $l = 0.83 \lambda = 20.75 \text{ mm}$. The antenna array with elements at the distance of 0.83λ has a dominant side lobe that is nearer to the main beam than other lobes. Therefore, the position of antenna array SLS is nearer to the main radiation beam. Furthermore, the intensity of the antenna array gain is satisfactory.

When radiating elements are positioned at the uniform distance of $l = 0.83 \lambda = 20.75 \text{ mm}$, the largest antenna dimension is $D = (n-1)l$, where n is the number of the radiating elements. If the usual formula $L = 2D^2/\lambda$ is used, the border between the far and near field zone equals $L_8 = 1.687 \text{ m}$ for an array with 8 radiating elements. The elements at the corner of the antenna array have a 50 times bigger phase error than the elements in the array center due to their positions. If the phase errors from certain array elements, which depend on the distance of the measuring antenna, are inputted into LINPLAN [2] software, the radiation pattern of the observed antenna is calculated at the determined distance.

The following distributions will be considered: Dolph-Chebyshev, Taylor and cosine's. It is important to appropriately select the parameters of the printed antenna array in order to make its realization possible through the use of the standard photolithographic process. The radiation elements are fed by the intensity determined by the mentioned distribution [2]. Side lobe suppressions are great (Ultralow side lobes), i.e., below -40 dB .

The antenna array with the Dolph-Chebyshev distribution of 2.2 orders has a pedestal of -19 dB . The expected side lobe suppression is 44.8 dB at position $\pm 19^\circ$. **Table 1** gives the feed intensity for the array's radiating elements.

Table 1
Feed intensities for radiating elements of the array with Dolph-Chebyshev distribution.

Elements number	1.	2.	3.	4.
	8.	7.	6.	5.
Feed intensity	0.12	0.387	0.742	1

Table 2 displays side lobe suppressions at distances that are multiples of L_8 , including phase errors that result from the antenna's radiating elements due to the distance of the measuring antenna from the radiation source.

Table 2

Side lobe suppression of the antenna array with Dolph-Chebyshev distribution, including phase errors from array elements.

Measuring antenna distance	SLS [dB]	Position [°]
L_8	-42.89	± 73.5
$2L_8$	-44.36	± 75
$3L_8$	-44.66	± 75
$4L_8$	-43.40	± 18
$5L_8$	-43.96	± 18.5
$6L_8$	-44.26	± 19
$7L_8$	-44.39	± 19

Fig. 3 shows the radiation patterns of the considered array at distance L_8 and distance $7L_8$ with and without studying the expected phase errors that originate from certain array elements, dependent on the distance of the measuring antenna. The radiation pattern corresponding to the usual distance L_8 shows deviations from the expected value and the positions of side lobe suppression when the phase errors from certain radiation elements are included. The radiation pattern corresponding to distance $7L_8$ shows only the deviations from the expected value of side lobe suppression, which is less than 1% in this case. Observing Fig. 3 can result in defining distance $7L_8$ as the border between the far and near field zone for the considered antenna array.

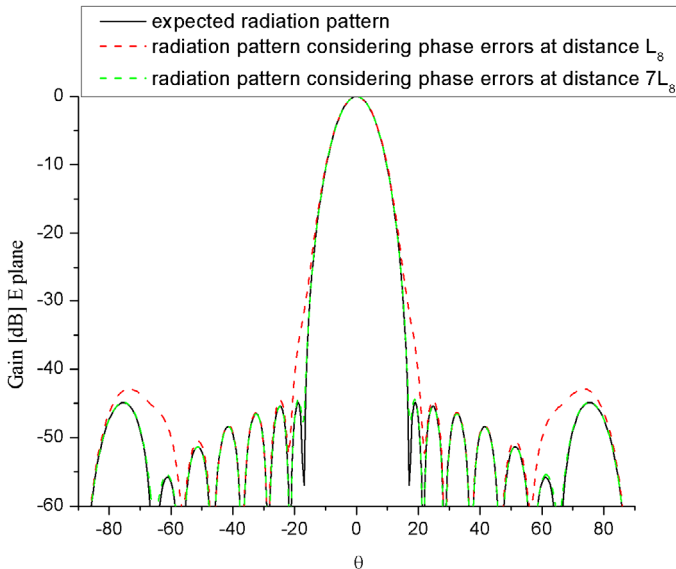


Fig. 3 – Radiation pattern at distance L_8 and at distance $7L_8$ including and excluding the expected phase errors for an antenna array with Dolph-Chebyshev distribution.

In addition, we will investigate the antenna array with the Taylor distribution of 2.2 orders, coefficient $\tilde{n} = 6$ and pedestal of -19 dB. The antenna array has a side lobe suppression of -44.93 dB at position $\pm 24.5^\circ$. The feed intensity for the radiating elements of the considered array can be seen in **Table 3**.

Table3

Feed intensities for the radiating elements of the array with Taylor distribution.

Elements number	1.	2.	3.	4.
	8.	7.	6.	5.
Feed intensity	0.122	0.388	0.742	1

Table4

Side lobe suppression of the antenna array with the Taylor distribution, including the phase errors from array elements.

Measuring antenna distance	SLS [dB]	Position [$^\circ$]
L_8	-42.94	± 73.5
$2L_8$	-44.44	± 75
$3L_8$	-44.74	± 75
$4L_8$	-44.03	± 18.5
$5L_8$	-44.65	± 18.5
$6L_8$	-44.93	± 24.5

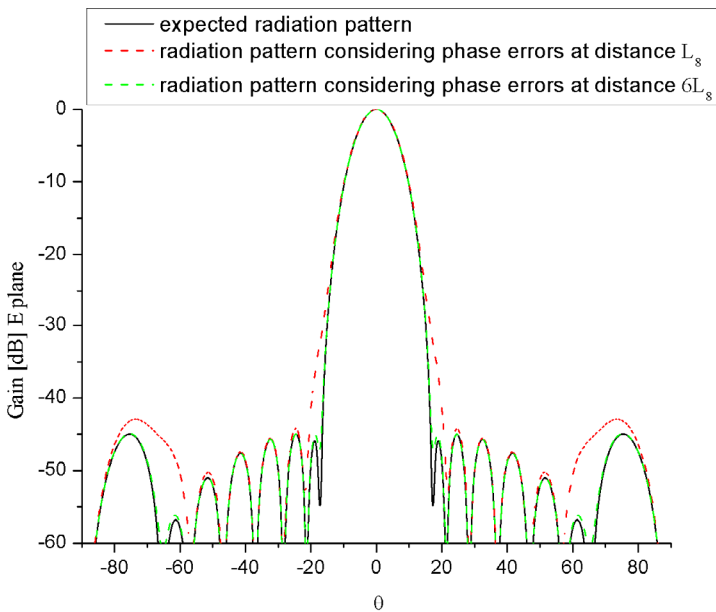


Fig. 4 – Radiation pattern at distance L_8 and at distance $6L_8$ including and excluding the expected phase errors for the antenna array with Taylor distribution.

Table 4 shows side lobe suppressions at distances that are multiples of L_8 , including the phase errors that result from the antenna radiating elements due to the distance of the measuring antenna from the radiation source.

Fig. 4 shows the radiation patterns of the considered array at distance L_8 and at distance $6L_8$ with and without studying the expected phase errors that originate from certain array elements, depending on the distance of the measuring antenna. Based on **Table 4** and Fig. 4, the border between the far and near field zone for the antenna array of 8 radiating elements with Taylor distribution is determined as $6L_8$.

The array with cosine's distribution of 2.1 orders has a side lobe suppression of -42.47 dB at position $\pm 31.5^\circ$. **Table 5** gives feed intensities for the radiating elements of the observed array.

Table 5

Feed intensities for the radiating elements of the array with cosine's distribution.

Elements number	1.	2.	3.	4.
	8.	7.	6.	5.
Feed intensity	0.112	0.36	0.73	1

Table 6 shows side lobe suppressions at distances that are multiples of L_8 , including phase errors that result from the antenna radiating elements of the observed antenna array with cosine's distribution. Based on **Table 6**, distance $2L_8$ can be determined as the border between the far and near field zone for an antenna array of 8 radiating elements with cosine's distribution.

Table 6

Side lobe suppression of the antenna array with cosine's distribution, including phase errors from array elements.

Measuring antenna distance	SLS (dB)	Position ($^\circ$)
L_8	-41.56	± 73
$2L_8$	-42.54	± 31.5

Fig. 5 shows the radiating patterns at distance L_8 and at distance $2L_8$ with and without studying expected phase errors that originate from certain array elements, depending on the distance of the measuring antenna.

The paper further investigates the antenna array with 10 and 12 radiating elements positioned at distance $l = 0.83 \lambda = 20.75$ mm. The theoretical value of the border between the far and near field zone equals $L_{10} = 2.79$ m for an array with 10 radiating elements and $L_{12} = 4.168$ m for an array with 12 radiating elements. Three distributions will be considered: Dolph-Chebyshev, Taylor and

cosine's. The pedestal is always -19 dB. The borders between the far and near field zone for an antenna array of 10 radiating elements and for an antenna array of 12 radiating elements are presented in **Table 7** and **Table 8**, respectively.

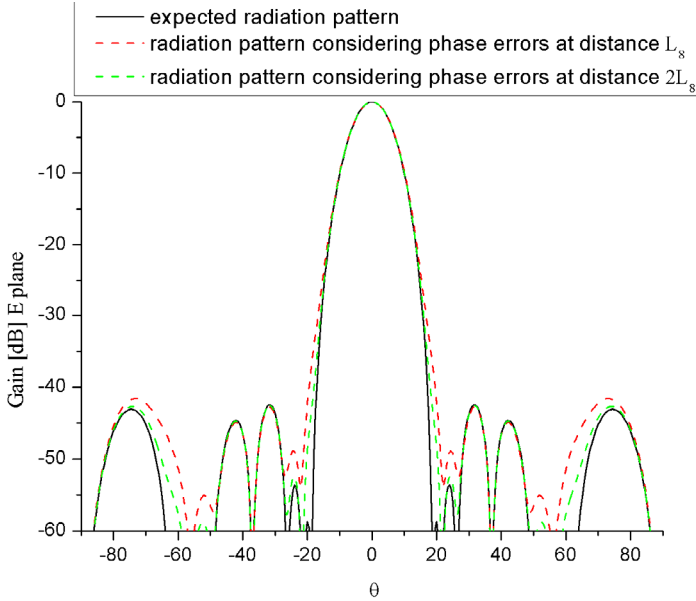


Fig. 5 – Radiation pattern at distance L_8 and at distance $2L_8$ including and excluding the expected phase errors for the antenna array with cosine's distribution.

Table 7

Border between the far and near field zone of the antenna array with 10 radiating elements, including phase errors.

Distribution	Border between the far and near field zone	SLS [dB]	Position [°]
Dolph-Chebyshev	L_{10}	-42.28	± 19
Taylor	$2L_{10}$	-42.62	± 25.5
Cosine's	L_{10}	-38.74	± 24.5

Table 8

The border between the far and near field zone of the antenna array with 12 radiating elements, including phase errors.

Distribution	Border between the far and near field zone	SLS [dB]	Position [°]
Dolph-Chebyshev	$5L_{12}$	-40.49	± 15.5
Taylor	L_{12}	-40.82	± 21.0
Cosine's	L_{12}	-37.96	± 20.5

3.2 Influence of the distance between array elements on the definition of the border between the far and near field zone

The investigation involves the antenna array with the Dolph-Chebyshev distribution of 2.2 orders and pedestal of -19 dB. The number of radiating elements n is changeable: $n = 8, 10$ and 12 . The theoretical formula for the border between the far and near field zone is $L'_n = 2D^2/\lambda$, where $D = (n-1)l$ is the largest dimension of the antenna array.

Table 9 presents the dependences of the border between the far and near field zone upon the distance between the array elements from $l \in [0.5 \lambda, 0.83 \lambda]$. Based on **Table 9**, it can be concluded that the border between the near and far radiation zone of the analyzed antenna increases in proportion with its largest dimension square $D = (n-1)l$.

Table 9
The dependences of the border between the far and near field zone upon the distance between the array elements.

The distance between the array elements [mm]	The border between the far and near field zone [m]		
	8 elements	10 elements	12 elements
$12.50 = 0.50 \lambda$	$4.287 = 7 L_8^{0.50}$	$1.012 = L_{10}^{0.50}$	$1.512 = L_{12}^{0.50}$
$13.25 = 0.53 \lambda$	$4.817 = 7 L_8^{0.53}$	$1.138 = L_{10}^{0.53}$	$1.699 = L_{12}^{0.53}$
$14.00 = 0.56 \lambda$	$5.378 = 7 L_8^{0.56}$	$1.270 = L_{10}^{0.56}$	$1.897 = L_{12}^{0.56}$
$14.75 = 0.59 \lambda$	$5.970 = 7 L_8^{0.59}$	$1.410 = L_{10}^{0.59}$	$2.106 = L_{12}^{0.59}$
$15.50 = 0.62 \lambda$	$6.592 = 7 L_8^{0.62}$	$1.557 = L_{10}^{0.62}$	$2.325 = L_{12}^{0.62}$
$16.25 = 0.65 \lambda$	$7.245 = 7 L_8^{0.65}$	$1.711 = L_{10}^{0.65}$	$2.556 = L_{12}^{0.65}$
$17.00 = 0.68 \lambda$	$7.930 = 7 L_8^{0.68}$	$1.873 = L_{10}^{0.68}$	$2.797 = L_{12}^{0.68}$
$17.75 = 0.71 \lambda$	$8.645 = 7 L_8^{0.71}$	$2.041 = L_{10}^{0.71}$	$3.050 = L_{12}^{0.71}$
$18.50 = 0.74 \lambda$	$9.391 = 7 L_8^{0.74}$	$2.218 = L_{10}^{0.74}$	$3.313 = L_{12}^{0.74}$
$19.25 = 0.77 \lambda$	$10.682 = 7 L_8^{0.77}$	$2.400 = L_{10}^{0.77}$	$3.587 = L_{12}^{0.77}$
$20.00 = 0.80 \lambda$	$10.976 = 7 L_8^{0.80}$	$2.592 = L_{10}^{0.80}$	$3.872 = L_{12}^{0.80}$
$20.75 = 0.83 \lambda$	$11.815 = 7 L_8^{0.83}$	$2.790 = L_{10}^{0.83}$	$20.839 = 5L_{12}^{0.83}$

3.3 Influence of the number of array elements on the definition of the border between the far and near field zone

The elements of the antenna array are positioned at an equal distance of $l = 20.75 \text{ mm} = 0.83 \lambda$. Three distributions are considered: Dolph-Chebyshev, of 2.2 orders, Taylor distribution, of 2.2 order, and coefficient $\tilde{n} = 6$, as well as cosine's distribution. The pedestal is always -19 dB. The theoretical formula for the border between the far and near field zone is $L_n = 2D^2/\lambda$, where $D = (n-1)0.83 \lambda$ is the biggest dimension of the antenna array.

Table 10 gives the dependences of the border between the far and near field zone upon the number of array elements. The dependence, presented in **Table 10**, is very random.

Table 10
The dependences of the border between the far and near field zone upon the number of array elements.

The number of array elements	The border between the far and near field zone [m]		
	Dolph-Chebyshev	Taylor	Cosine's
8	$11.815 = 7L_8$	$10.127 = 6L_8$	$3.370 = 2L_8$
9	$2.2 = L_9$	$2.2 = L_9$	$2.200 = L_9$
10	$2.79 = L_{10}$	$5.580 = 2L_{10}$	$2.790 = L_{10}$
11	$3.445 = L_{11}$	$3.445 = L_{11}$	$3.445 = L_{11}$
12	$20.839 = 5L_{12}$	$4.168 = L_{12}$	$4.168 = L_{12}$
13	$4.96 = L_{13}$	$4.96 = L_{13}$	$4.960 = L_{13}$
14	$11.642 = 2L_{14}$	$5.821 = L_{14}$	$5.821 = L_{14}$

4 The Concept and Characteristics of the Printed Antenna with High Side Lobe Suppression

The antenna array, shown in Fig. 2, is realized. It consists of 3 parts: linear array with 8 pentagonal dipoles, feed network and reflector plane. The linear array of 8 dipoles is on the substrate of dielectric electrical constant 2.1, height of 0.508 mm and length of 166 mm. The dipole dimension was optimized with WIPL-D software [4] to adjust its impedance to 100 Ω at the central frequency of 12 GHz. The dipoles are positioned at the distance of 20.75 mm = 0.83 λ. The reflector plane, in the dimensions of (240×52) mm, is situated at distance λ/4 = 6.25 mm from the planar array (Fig. 2). The array is realized using the Dolph-Chebyshev distribution of 2.2 orders and pedestal of -19 dB. The feed coefficients calculated by LINPLAN [2] software have the following values: A1 = A8 = 0.12, A2 = A7 = 0.387, A3 = A6 = 0.742 and A4 = A5 = 1.

Due to the tolerances in the photolithographic process, there is an occurrence of deviations from the projected values of position, amplitude and phase of the array's radiating elements. The expected tolerances in the standard photolithographic process have been assumed with moderate precision in order to estimate SLS degradation, due to the amplitude and phase deviations, as well as radiating element positioning deviations from the optimized values.

Realizable values of relative tolerances have been assumed at the operating frequency of 12 GHz. There are two types of tolerances:

- real case (b) when the deviations in distances between the radiating elements in the array are 1 % of λ , amplitude deviations along the tapered feeding lines are 1 dB and phase deviations are 0.908° , corresponding to approximately $40 \mu\text{m}$;
- the worst case (c) when the deviations in the distances between the radiating elements in the array are 2% of λ , amplitude deviations along the tapered feeding lines are 2 dB and phase deviations are 1.835° , corresponding to approximately $80 \mu\text{m}$.

The expected deviations from the projection value are presented in **Table 11**.

Table 11
Deviation due to the tolerances in the photolithographic process.

	Deviation			SLS – position
	position	amplitude	phase	
a	0	0	0	$-44.80 \text{ dB} \pm 19^\circ$
b	0.005	1%	0.908	$-41.90 \text{ dB} \pm 24.5^\circ$
c	0.01	2%	1.835	$-39.34 \text{ dB} \pm 25^\circ$

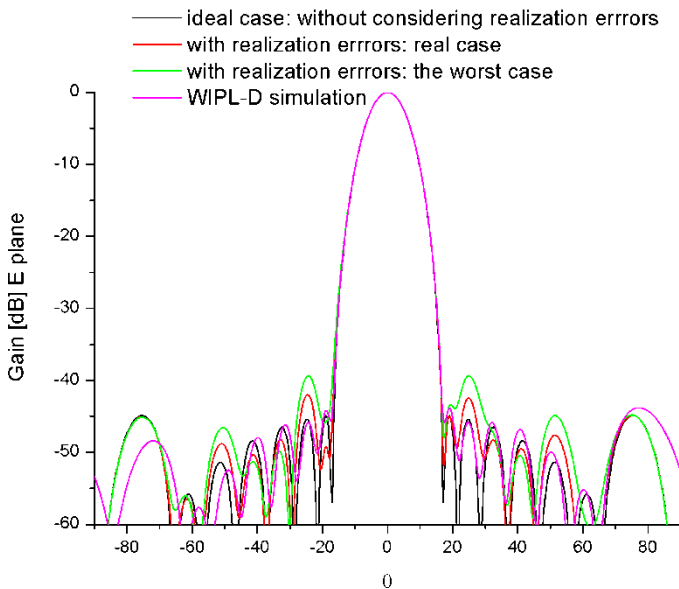


Fig. 6 – Antenna array radiation pattern, including realization errors.

Fig. 6 shows the radiation pattern of the considered antenna array obtained by LINPLAN [2] and WIPL-D [4] software. LINPLAN [2] allows the generation radiation pattern, including and excluding the realization errors (Fig. 6).

5 Conclusion

The experimental verification of the radiation pattern of an antenna array requires the necessary measurement in the far field zone. The conventional formula $L = 2D^2/\lambda$ for the border between the far and near field zone, where D is the largest array dimension, is useless for side lobe suppression between 30 dB and 40 dB (Low sidelobe), as well as the side lobe suppression above 40 dB (Ultralow sidelobes). In these cases, the border between the far and near field zone can be the multiple of the theoretical border L .

Besides the applied distribution of the antenna array, the number of the radiating elements and their distance can influence the radiation pattern and position of the side lobes. Therefore, it is necessary to calculate the phase errors from a certain antenna's radiating elements to determine the actual border between the far and near field zone, where the radiating pattern is very close to the real radiating pattern. In addition, it is useful to consider the influences of tolerances in the photolithographic process on the position and values of the side lobe suppression of the antenna array.

6 Acknowledgement

This work was supported by the Ministry of Education, Science and Technology Development of Serbia within project no. TR32052.

7 References

- [1] P. Hacker, H. Schrank: Range Distance Requirements for Measuring Low and Ultralow Sidelobe Antenna Patterns, IEEE Transactions on Antennas and Propagation, Vol. 30, No.5, Sept. 1982, pp. 956 – 966.
- [2] M. Mikavica, A. Nešić: CAD for Linear and Planar Antenna Array of Various Radiating Elements: Software And User's Manual, Artech House, Norwood, MA, USA, 1992.
- [3] J.D. Kraus: Antennas, 2nd Edition, McGraw-Hill, NY, USA, 1988.
- [4] WIPL-D Pro v9.0, WIPL-D Team.